MULTIRESOLUTION TARGET DETECTION IN SAR IMAGERY

Nikola S. Subotic, Leslie M. Collins, John D. Gorman, and Brian J. Thelen

Environmental Research Institute of Michigan
P.O. Box 134001
Ann Arbor, MI 48113-4001
Telephone:(313)-994-1200
email: subotic@erim.org

ABSTRACT

We demonstrate the utility of a multiresolution approach for target detection in SAR imagery. Man-made objects exhibit characteristic phase and amplitude fluctuations as the image resolution is varied, while natural terrain has a random signature. We construct a number of detection strategies: an optimal invariant multiresolution detector based on a derived multiresolution increments process; and a generalized likelihood ratio detector to differentiate between a first-order autoregressive multiresolution increments process and white noise. We show that these schemes significantly outperform a standard energy detector operating on the finest available SAR resolution.

1. INTRODUCTION

Many synthetic aperture radar (SAR) target detection algorithms work on a single resolution image at the finest available resolution [4]. However, there is compelling evidence to suggest that significant performance gains can be achieved by casting the detection problem in a multiresolution setting. This performance gain is a direct result of the coherent interference effects that occur in typical radar target signatures as the imaging resolution is varied.

SAR images of man-made objects typically consist of spatial patterns of bright points and lines resulting from radar backscatter from discrete physical features such as corners, edges, flat plates, etc. The coherent radar return from each of these discrete features, or *prominent scatterers*, is a complex phasor with amplitude equal to the local radar cross-section of the target feature. As the resolution changes from fine to coarse, adjacent scatterers become lumped together into a single resolution cell and coherently interfere with each other, leading to characteristic changes in amplitude and phase as a function of resolution.

Figure 1 shows three collinear scatterers each of equal amplitude and separated by a distance D. Also shown are the amplitude and phase of a pixel located at the origin, plotted as a function of resolution. One can see that coherent interference effects cause the pixel amplitude and phase to oscillate as the resolution is varied from fine to coarse.

Natural terrain typically consists of a large collection of small amplitude scatterers that are randomly distributed within each resolution cell. Thus SAR imagery of terrain, i.e., *clutter*, is frequently modeled as a Gaussian random field by appealing to the law of large numbers [7]. The result is that the amplitude and phase of a clutter pixel vary randomly as a function of resolution.

2. MULTIRESOLUTION PROCESS STATISTICS

In our construction, we model the scene $c(\underline{x})$, $\underline{x} \in \mathbb{R}^2$ as a collection of point scatterers, in which each point scatterer is specified by its location $\underline{x}_k \in \mathbb{R}^2$ and complex reflectivity $u_k \in \mathbb{C}$:

$$c(\underline{x}) = \sum_{k=1}^{K} u_k \delta(\underline{x} - \underline{x}_k). \tag{1}$$

This approach has been used to model both clutter and objects that consist of collections of point reflectors [7, and references therein] (i.e., trihedrals or corner reflectors). We refer to c as the complex reflectivity function.

The complex-valued SAR image, $T(\underline{x}; \rho)$, taking into account resolution, can be written as a convolution between the complex reflectivity function, $c(\underline{x})$,

This research supported by ARPA/STO contract DAAH01-93-C-R346.

0-7803-2431-5/95 $4.00

and the system impulse response, $h(\underline{x})$, [8]:

$$T(\underline{x};\rho) = \frac{1}{\rho}\int c(\underline{y})h\left(\frac{\underline{x}-\underline{y}}{\rho}\right)d\underline{y} \qquad (2)$$

In the next two sections, we consider models for the statistics of the observed radar image, T, under simple assumptions on the statistics of the scatterer locations $\{\underline{x}_k\}$ and their complex reflectivities $\{u_k\}$.

2.1. Case 1: Natural Clutter

For natural terrain, i.e., *clutter*, a typical assumption is that each resolution cell in the SAR image contains a large number of small amplitude scatterers. In this case, we will assume that the complex reflectivities $\{u_k\}$ are independent, identically distributed (*iid*) random variables with mean zero and covariance $\sigma_c^2 I$ where I is the identity matrix.

Using a slight generalization of a result in [7], we can invoke the Generalized Multivariate Central Limit Theorem [1] to show that the joint density of $T(\underline{x};\rho)$ converges to multivariate Gaussian as the number of scatterers K tends to infinity. in both space and resolution. The mean of the process is 0 and the covariance is

$$E\{T(\underline{x};\rho)T^*(\underline{x}';\rho')\} = R(\underline{x},\underline{x}';\rho,\rho')$$
$$= \frac{\sigma_c^2}{\rho\rho'}\int h\left(\frac{\underline{x}-\underline{y}'}{\rho}\right)h^*\left(\frac{\underline{x}'-\underline{y}'}{\rho'}\right)dy', \qquad (3)$$

where $R(\underline{x},\underline{x}';\rho,\rho')$ is the correlation function of $T(\underline{x},\rho)$, and σ_c is the variance of the iid complex reflectivities $\{u_k\}$. Note that the covariance function is completely specified by the variance σ_c and the impulse response $h(\underline{x})$.

If the impulse response is chosen so that the correlation function R satisfies a scaling law condition [9] with respect to resolution, then the process $T(\underline{x};\rho)$ is Gauss-Markov in resolution. For $\rho_l \le \rho \le \rho_u$ the scaling law is

$$R_{\underline{x}_0}(\rho_l,\rho_u) = \frac{R_{\underline{x}_0}(\rho_l,\rho)R_{\underline{x}_0}(\rho,\rho_u)}{R_{\underline{x}_0}(\rho,\rho)}. \qquad (4)$$

where $R_{\underline{x}_0}(\rho,\rho') = R(\underline{x}_0,\underline{x}_0;\rho,\rho')$.

For the special case where either the impulse response $h(\underline{x})$ is a sinc$(\underline{x})$ or a rect$(\underline{x})$, the scaling relation is satisfied. The correlation of $T(\underline{x}_0;\rho)$ becomes $R_{\underline{x}_0}(\rho,\rho') = \sigma_c^2/max\{\rho,\rho'\}$ with variance $\sigma^2 = \sigma_c^2/\rho$.

$T(\underline{x};\rho)$ can also be shown to have independent increments in resolution – i.e.

$$E\{[T(\underline{x}_0,\rho_1) - T(\underline{x}_0,\rho_2)][T(\underline{x}_0,\rho_2) - T(\underline{x}_0,\rho_3)]^*\} = 0 \qquad (5)$$

for $\rho_1 > \rho_2 > \rho_3$, . In this case, the clutter process $T(\underline{x}_0,\rho)$ is a Brownian motion process when viewed as a function of $\frac{1}{\rho}$ [5].

The Brownian motion nature of T in resolution can be exploited to provide a simple linear transformation of the process which whitens the process in resolution. Choose a set of resolutions $\rho_1 < \ldots < \rho_i < \rho_{i+1} < \ldots < \rho_N$ where $\rho_{i+1} = \rho_i + \delta\rho_i$. An increments process in resolution is formed by

$$T'(\underline{x}_0;\rho_i) = T(\underline{x}_0;\rho_i+\delta\rho_i) - T(\underline{x}_0;\rho_i) \qquad (6)$$

with $\delta\rho_i > 0$. This process has zero mean and is independent from resolution to resolution.

By judiciously choosing the resolutions $\{\rho_i\}$, so that $\frac{1}{\rho_i} - \frac{1}{\rho_{i+1}} = \gamma$ for every i, the variance of the difference process T' is constant from resolution to resolution. We define the vector of resolution increments

$$\underline{T}'_{\underline{x}_0} = \{T'(\underline{x}_0,\rho_1),\ldots,T'(\underline{x}_0,\rho_{N-1})\}^t \qquad (7)$$

where t denotes vector transpose. Then $\underline{T}'_{\underline{x}_0}$ has distribution $\underline{T}'_{\underline{x}_0} \sim \mathcal{N}_c(\underline{0},\gamma\sigma_c^2 I)$ where $\mathcal{N}_c(\underline{\mu},\Sigma)$ denotes a circular complex Gaussian density with mean $\underline{\mu}$ and complex covariance Σ. Here the symbol $\sim$ is shorthand notation for the phrase "has probability distribution."

2.2. Case 2: Statistics of Cultural Objects

Many man-made or cultural objects typically consist of a small number of large amplitude point scatterers. The number of local prominent scatterers we wish to examine are typically less than eight. Larger numbers tend to make the SAR signature exhibit zero mean complex Gaussian statistics [3].

We will reformulate the process to have a random and nonrandom component. The point scatterer model will become

$$c(\underline{x}) = \sum_{k=1}^{K} u_k\delta(\underline{x}-\underline{x}_k) + \sum_{k=1}^{K'} a_k\delta(\underline{x}-\underline{x}_k). \qquad (8)$$

The first term in Equation 8 will correspond to the clutter model as outlined in Case 1. The second term will correspond to an unknown set of prominent scatterers. The complex reflectivities $\{a_k\}$ are deterministic but unknown. The spatial distribution of the prominant scatterers is also assumed to be deterministic but unknown. $T(\underline{x};\rho)$ will be multivariate Gaussian with covariance as in Case 1 (Eq. 3). The mean of the process is

$$E\{T(\underline{x};\rho)\} = \frac{1}{\rho}\sum_{k=1}^{K'} a_k h\left(\frac{\underline{x}-\underline{x}_k}{\rho}\right). \qquad (9)$$

In the same spirit as Case 1, we form a vector of increments in resolution, $\underline{T'}_{\underline{x}_0}$. This process is complex Gaussian with distribution $\underline{T'}_{\underline{x}_0} \sim \mathcal{N}_c(\underline{\mu}, \gamma\sigma_c^2 I)$ where $\underline{\mu} = \{\mu_1, \ldots, \mu_i, \ldots, \mu_{N-1}\}^t$.

3. DETECTION STRATEGIES

We will base our detection strategies on the increments process $T'(\underline{x}_0; \underline{\rho})$. Our detection strategies will exploit information provided by resolution. This information is, in fact, produced by the local spatial signature as it is incorporated into the resolution process. The above developments motivate detectors which exploit the difference in the mean when either clutter or cultural objects are present. For a given spatial location $\underline{x}_0$,the hypotheses under test will be

$$\begin{aligned} H_0: &\ \underline{T'}_{\underline{x}_0} \sim \mathcal{N}_c(\underline{\mu}, \Sigma_{\underline{x}_0}), \quad \underline{\mu} = \underline{0} \\ H_1: &\ \underline{T'}_{\underline{x}_0} \sim \mathcal{N}_c(\underline{\mu}, \Sigma_{\underline{x}_0}), \quad \underline{\mu} \neq \underline{0} \end{aligned}$$

with $\Sigma_{\underline{x}_0} = \gamma\sigma_c^2 I$. We have available $\underline{T'}_{\underline{x}_j}\ j = 1, \ldots, M$ which are surrounding locations assumed to be clutter.

We have chosen the composite test due to the severe variability of SAR signatures when collection geometry and object condition are not known. This is opposed to choosing a specific object signature and designing a matched filter to it. There does not exist a uniformly most powerful test for the above composite hypothesis. The optimal invariant test with respect to scale and orthogonal transformations is the so-called F test [2] which is equivalent to

$$\psi_1(\underline{x}_0) = \frac{|\Sigma_{\underline{x}_0}^{-1/2}\underline{T'}_{\underline{x}_0}|^2}{N-1} = \sum_{i=1}^{N-1} \frac{|T'(\underline{x}_0; \rho_i)|^2}{(N-1)\gamma\hat{\sigma}_c^2} \overset{H_1}{>} \beta. \tag{10}$$

where $\hat{\sigma}_c^2$ is the estimate of σ_c^2 from surrounding cells assuming no target is present, i.e.,

$$\hat{\sigma}_c^2 = \frac{\sum_{i=1}^{N-1}\sum_{j=1}^{M}|T'(\underline{x}_j; \rho_i)|^2}{M(N-1)}. \tag{11}$$

where $\underline{x}_1, \ldots, \underline{x}_M$ are locations within clutter. The distribution of the test statistic is $\psi_1(\underline{x}_0) \sim F(2(N-1), 2M(N-1))$ under H_0, and $\psi_1(\underline{x}_0) \sim F(2(N-1), 2M(N-1); \sum_{i=1}^{N-1}(\mu_i^2/\gamma\sigma_c^2))$ under H_1. Here $F(m,n)$ is the central F distribution with m and n degrees of freedom, and $F(m,n;\eta)$ is the noncentral F distribution with the same degrees of freedom and noncentricity parameter η. For the case of large $M(N-1)$, the estimate of $\hat{\sigma}_c^2$ is almost exact. The distributions become a scaled central chi-square under H_0 and a scaled non-central chi-square under H_1.

An alternative detection strategy can be motivated by noting the oscillatory behavior in the signature of Figure 1. We now construct a generalized likelihood ratio test (GLRT) for the hypotheses

$$\begin{aligned} H_0: &\ T'(\underline{x}_0; \rho_i) = \epsilon_i \\ H_1: &\ T'(\underline{x}_0; \rho_i) = aT'(\underline{x}_0; \rho_{i-1}) + \epsilon_i \end{aligned}$$

where $\epsilon_i \sim \mathcal{N}_c(0, \gamma\sigma_c^2)$. We are now testing between a white noise process and a first order autoregressive (AR) process in resolution. The GLRT is developed through the inclusion of the maximum likelihood estimates of the AR coefficient a and σ_c^2 [1]. Assuming $M >> N$, the GLRT is approximated as

$$\psi_2(\underline{x}_0) = \frac{\left|\sum_{i=2}^{N} T'(\underline{x}_0; \rho_i)T'^*(\underline{x}_0; \rho_{i-1})\right|^2}{\hat{\sigma}_c^2 \sum_{i=2}^{N}|T'(\underline{x}_0; \rho_{i-1})|^2} \overset{H_1}{>} \beta. \tag{12}$$

Our baseline test with which we compare the multiresolution test performance is an F test applied to single resolution SAR image data at the finest resolution. This test is

$$\psi_3(\underline{x}_0) = \frac{|T(\underline{x}_0; \rho_N)|^2}{\hat{\sigma}_c^2} \overset{H_1}{>} \beta \tag{13}$$

This test has been used extensively in initial screening algorithms on SAR data[6]. The distribution of this test is the same as $\psi_1(\underline{x}_0)$ with $M = 1$, $N = 2$, and noncentricity parameter $\eta = |E\{T(\underline{x}_0; \rho_N)|H_1\}|^2/\sigma_c^2$.

We tested these detection strategies on a data set which consisted of 17 Synthetic Radar Imaging Model (SRIM) images of a Howitzer, each at a multiple of 20° aspect angle embedded in zero mean circular complex Gaussian clutter with σ_c^2 chosen such that the Target-to-clutter ratio was $0dB$. The resolution of this simulation is 1 foot. Figure 2 shows the Receiver Operating Characteristic of these tests when applied to this data set. Noted in the Figure is the test, finest/coarsest resolutions, and number of resolutions used. The multiresolution F-test performed the best in this study. Also note that the multiresolution F-test using 2 foot data as its finest resolution performed as well as or better than the single resolution F-test at 1 foot resolution.

4. CONCLUSION

In this paper we derived the statistics for multiresolution SAR signatures. For the clutter case we appealed to the Generalized Central Limit Theorem to show that the clutter statistics are complex Gaussian. In addition, we showed that under certain aperture

weighting conditions, the clutter process in resolution becomes Brownian motion. The Brownian motion process was exploited to simplify the clutter statistics by forming an increments process and by choosing the resolutions to equalize the clutter variance. A target model was presented where a deterministic but unknown set of point scatterers were added to the marked point process clutter model. Two multiresolution detection strategies are proposed to detect cultural objects whereby the mean value of the objects is not assumed known. An optimal invariant test and a test for autoregressive behavior were explored and found to outperform a simple fine resolution energy detector.

5. REFERENCES

[1] T. W. Anderson, *An Introduction to Multivariate Statistical Analysis, 2nd Edition,* Wiley, 1984.

[2] S. F. Arnold, *The Theory of Linear Models and Multivariate Analysis,* Wiley, 1981.

[3] P. Beckman, and A. Spizzichino, *The Scattering of Electromagnetic Waves From Rough Surfaces,* Artech House, Norwood, MA (1987).

[4] G. Minler and J. Minkler, *CFAR: The Principles of Automatic Radar Detection in Clutter,* Magellan, Baltimore, 1990.

[5] Papoulis, A., *Probability, Random Variables and Stochastic Processes,* McGraw-Hill, New York, (1965).

[6] S. R. Sullivan, et. al., "Strategic Target Algorithm Research (STAR) - Final Report," Contract Number F19628-90-C-0002, 1991, SECRET.

[7] B. J. Thelen, "Complete Characterization of Complex Distributions from Weak Scatterers, *J. Opt. Soc. Amer., ser. A,* in review, 1994.

[8] Walker, J. L., "Range-Doppler Imaging of Rotating Objects," *IEEE Trans. Aerosp. Electron. Syst.,* vol. **AES- 16**, p. 23, Jan. 1980.

[9] Wong, E., and Hajek, B., *Stochastic Processes in Engineering Systems,* Springer, Berlin, (1985).

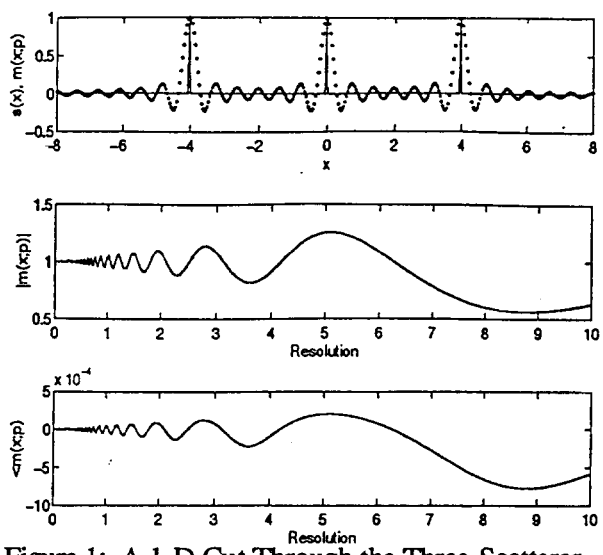

Figure 1: A 1-D Cut Through the Three-Scatterer Signal and Multiresolution Amplitude and Phase Fluctuations.

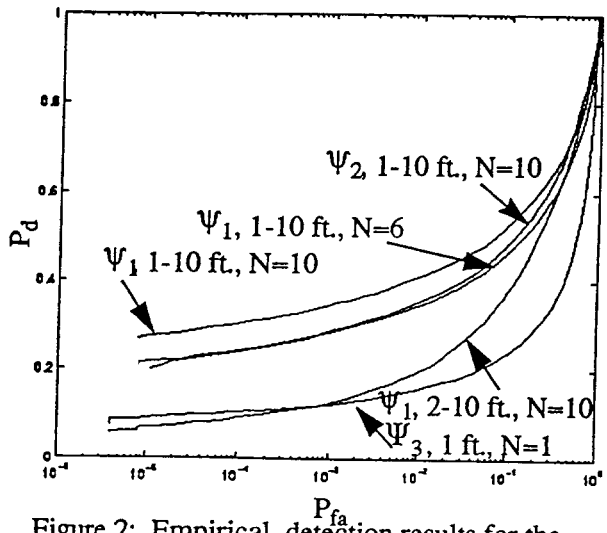

Figure 2: Empirical detection results for the three detection strategies on synthetic data